

An efficient strategy to describe the propagation of variation through multi-stage metal forming processes

B.M. de Gooijer¹, J. Hazrati-Marangalou¹, H.J.M. Geijselaers¹, A.H. van den Boogaard¹

¹ University of Twente, Chair of Nonlinear Solid Mechanics

Drienerlolaan 5, 7522 NB, Enschede, The Netherlands

e-mail: b.m.degooijer@utwente.nl

Abstract

In this work an efficient strategy to describe the propagation of uncertainty throughout a production process is proposed and validated. A two-stage metal forming process is used to demonstrate the proposed strategy. A metamodel of the first stage is built using a singular value decomposition combined with multiquadric radial basis functions. The strategy is validated by comparing the propagated results from the first stage, of both the metamodel and a finite element model, to a second stage finite element model for a new set of validation points. Using the proposed strategy, it will be possible to efficiently optimize multi-stage processes under uncertainty.

1 Introduction

When the uncertainties in a production process are in the same order of magnitude as the desired product tolerances, these uncertainties must be taken into consideration in order to design products that meet a required accuracy [1, 2]. Robust optimization is commonly used to design products or processes whilst taking into account the manufacturing variability. However an efficient strategy to optimize multi-stage processes is still lacking.

In robust optimization one can distinguish two types of variables [3, 4]: noise variables that cause process uncertainty (e.g. material scatter, machine dynamics or temperature changes) and design variables that can be set by a designer or operator (e.g. tooling geometry or machine settings).

The goal of robust optimization is to find the set of design variables that minimizes the uncertainty in an objective function. However, with an increasing number of process stages, the dimensionality of the problem at hand increases as well. Because of this high dimensionality, optimizing all process stages at once will not be efficient. One solution is to optimize each process stage separately. However, as shown by Suri & Otto [5] this approach will most certainly not lead to the global optimum after the last process stage. Thus, in order to be able to solve the robust optimization problem at hand, variation must be propagated from one stage to the next. To do so efficiently, numerical techniques such as metamodeling and decomposition methods can be applied.

The first attempt in optimization of a multi-stage metal forming process, although deterministic, was done by Roy et al. [6]. In their work all process stages are optimized simultaneously. In this approach the entire production chain is treated as a single stage. Other deterministic optimizations that use a simultaneous approach can be found in [7-10]. Kusiak, Jarosz et al. [11, 12] separate the simultaneous approach into sequential deterministic optimization of each stage for different levels of aggregation. Steffes-lai [13] and Sun [14] et al. show the importance of taking into account the forming history by comparing physical experiments with computer analyses. Du & Chen [15] propose two different approaches for describing the propagation of uncertainty through the process stages, which are an extreme condition approach and a statistical approach.

In this work, an efficient strategy to describe the propagation of uncertainty throughout the production process is proposed and validated. In Section 2, a general description of a production process is suggested

first. After that, a strategy is proposed to describe the propagation of uncertainty from one process stage to the next as low-dimensional as possible. In Section 3, a demonstrator process is introduced to validate the proposed strategy. The results of the first stage of the demonstrator process, of both a metamodel and a finite element model, are propagated to the second stage finite element model for a new set of validation points. Using the proposed strategy, it will be possible to efficiently optimize multi-stage processes under uncertainty.

2 Strategy for describing the propagation of variation

2.1 General description of a multi-stage production process

Before describing the strategy for propagation of variation, first a general description of a production process is suggested. A schematic representation of a two stage production process is given in Figure 1. Note however, that the description can be extended to an indefinite number of stages.

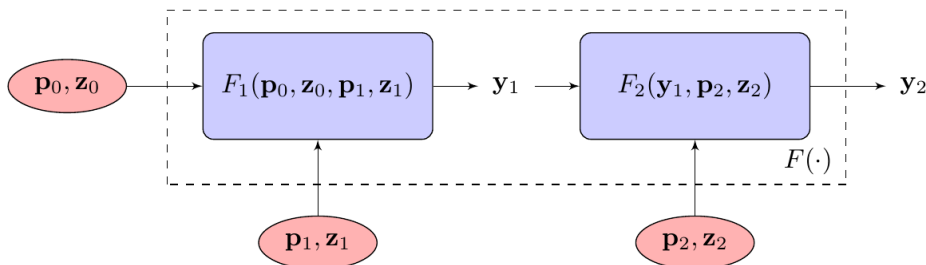


Figure 1: Schematic representation of a two stage production process.

When describing a production process two types of input variables can be distinguished: noise variables and design variables, denoted with z and p respectively. The vectors containing all noise and all design variables corresponding to process stage i are denoted with \mathbf{z}_i and \mathbf{p}_i respectively. Each process stage is a function of the output of the previous stage \mathbf{y}_{i-1} and its noise and design variables, hence $F_i(\mathbf{y}_{i-1}, \mathbf{p}_i, \mathbf{z}_i)$. One exception for this is the first stage, where the process stage is a function of the initial variables, indicated with subscript 0, and its corresponding noise and design variables. Initial design variables are generally discrete, e.g. material type or thickness [1]. Noise variables are usually continuous and can be modelled with different types of distributions, e.g. normal, uniform or skewed distributions. Note that if there is a noise variable in the input, the output of all subsequent stages has to be considered as noise with an undetermined distribution. This output distribution can be determined by means of e.g. Monte Carlo sampling or analytical methods as proposed by Nejadseyfi et al. [16].

The goal of a robust optimization is to find the set of design variables $\{\mathbf{p}_1, \dots, \mathbf{p}_N\}$ that minimizes the sensitivity of the objective with respect to the noise variables or that minimizes an objective function under the constraint of sufficient robustness. The objective function will be a function of the output of the final stage $f_{obj}(\mathbf{y}_N)$, e.g. attaining a geometrical requirement or preventing defects such as wrinkling or fracture. Besides approaching each stage as a separate function $F_i(\cdot)$, one can define a function describing the entire production process $F(\cdot)$. In this simultaneous approach, all stages are combined to one single stage with a large number of design and noise parameters. Due to the high-dimensionality of the problem at hand, it will be infeasible to find an optimum using this simultaneous approach. Hence, in order to analyze the variation at the final stage and optimize the multi-stage production process under uncertainty, one needs to efficiently describe each process stage.

2.2 Efficiently propagating variation through multi-stage production processes

To efficiently describe a process stage, the variation in output of the stage must be captured as low-dimensional as possible. The strategy to efficiently describe the output of stage i consists of 3 steps:

1. Obtain training set of stage i

Based on a sampling method or a combination of sampling methods, a set of K sample points $\{\mathbf{z}_i, \mathbf{p}_i\}^{(k)}$ needs to be generated. Examples of sampling methods are full/fractional factorial design, central composite design, Latin hypercube sampling or a Halton/Sobol sequence. At each point k in the set the stage i model must be evaluated to obtain the output training data.

2. Reduce output of stage i

To find the dominant behavior in the training data of the i^{th} -stage output, a singular value decomposition (SVD) is applied. In a SVD a new geometric space is sought that maximizes the variation along its new axes [17]. In order to apply SVD, each output in the set of training data of stage i must be stored in a column vector $\mathbf{y}_i^{(k)}$. All K column vectors are collected in a so-called snapshot matrix \mathbf{Y}_i [16, 17]:

$$\mathbf{Y}_i = [\mathbf{y}_i^{(1)} \quad \dots \quad \mathbf{y}_i^{(K)}] \quad (1)$$

Now the snapshot matrix can be decomposed using SVD:

$$\mathbf{Y}_i = \mathbf{\Phi} \mathbf{S} \mathbf{V}^T \quad (2)$$

Herein \mathbf{S} is a diagonal matrix containing the K real positive singular values s_k in descending order, $\mathbf{\Phi}$ is a matrix with the left-singular vectors $\boldsymbol{\phi}_k$ as its columns and \mathbf{V} is a matrix with the right-singular vectors \mathbf{v}_k as its columns. Note that $\mathbf{\Phi}$ has the same size as \mathbf{Y}_i , whereas \mathbf{V} has size K by K . A new truncated basis $\bar{\mathbf{\Phi}}$ can be constructed from the first N_s right-singular vectors.

As $\mathbf{\Phi}$ is an orthogonal matrix, the amplitudes \mathbf{A} corresponding to the K outputs vectors can be found by projecting the snapshot matrix \mathbf{Y}_i in the new basis:

$$\mathbf{A} = \bar{\mathbf{\Phi}}^T \mathbf{Y}_i \quad (3)$$

Now each output in the training set can be approximated by multiplying the truncated basis with the corresponding column of the amplitude matrix $\mathbf{a}^{(k)}$ consisting of the N_s amplitudes corresponding to sample point k .

$$\mathbf{y}_i^{(k)} \approx \bar{\mathbf{\Phi}} \mathbf{a}^{(k)} \quad (4)$$

3. Build metamodel of output stage i

In order to build a metamodel of the i^{th} -stage output, the N_s amplitudes need to be interpolated. This can be done using e.g. Kriging, Radial Basis Functions or Response Surface Methods.

Using the obtained metamodel the output of stage i can be propagated to the next stage efficiently. This strategy can be repeated until the last stage is reached. When the metamodels of all stages are obtained, they can be used to solve the robust optimization problem.

3 Two-stage demonstrator process

To demonstrate the strategy proposed in the previous Section, a two-stage metal forming process is considered. A nonlinear, plane strain Finite Element (FE) model of both stages is constructed using the FE software MSc Marc and its preprocessor Mentat. In the first process step a sheet metal workpiece is bent downwards, where after it is bent upwards in the second step. A schematic representation of the FE model is presented in Figure 2. The sheet metal is meshed using 1200 quadrilateral elements (N_{elem}) and 1296 nodes (N_{nod}). The elements are fully integrated using four integration points ($N_{ip} = 4 \cdot N_{elem} = 4800$).

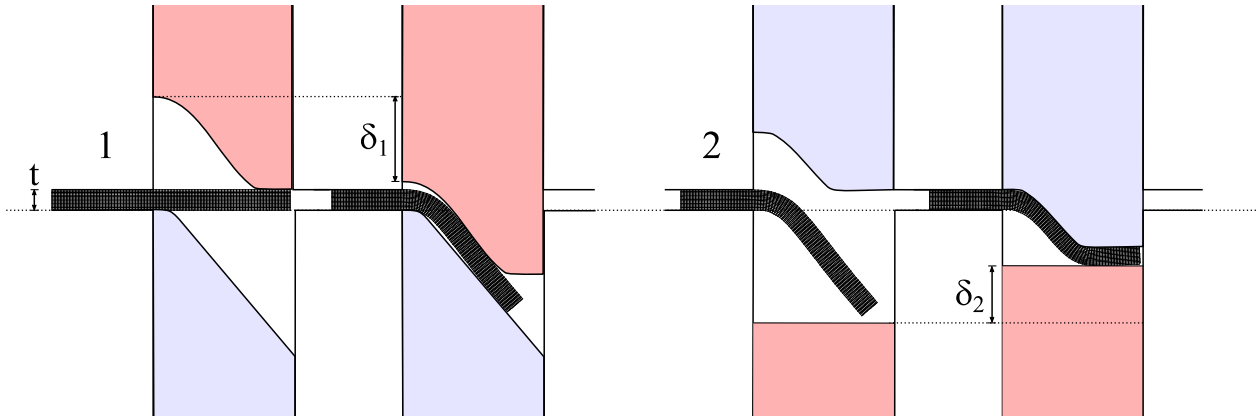


Figure 2: Schematic representation of the two stage FE model.

Following the general description as suggested in Section 2.1, there are only three parameters of interest among all model parameters. The vector with initial noise parameters \mathbf{z}_0 , only contains the thickness t of the sheet metal. Hence:

$$\mathbf{z}_0 = \{t\} = 0.300 \pm 0.005 \text{ mm} \quad (5)$$

The vector with the design parameters of the first stage \mathbf{p}_1 , only contains the punch end distance δ_1 :

$$\mathbf{p}_1 = \{\delta_1\} = 1.55 \pm 0.05 \text{ mm} \quad (6)$$

For ease of notation the noise and design parameter are combined to a 2 dimensional parameter space:

$$\mathbf{x} = \{t, \delta_1\} \quad (7)$$

In the second stage no noise parameters are considered. Note however, that the uncertainty from the initial noise parameter will propagate to the second stage through the output \mathbf{y}_1 . The vector with the design parameters of the second stage \mathbf{p}_2 , only contains the punch end distance δ_2 :

$$\mathbf{p}_2 = \{\delta_2\} = 2.1 \pm 0.1 \text{ mm} \quad (8)$$

3.1 Obtaining the first stage training set

To sample the first stage, a Latin hypercube sampling is used. According to Steffes-Lai [13] the number of training points needed in a D -dimensional parameter space can be calculated using:

$$K = 2 \left[2 + D + \frac{D(D+1)}{2} \right] \quad (9)$$

Which results in 14 training points $\mathbf{x}^{(k)}$ for the first stage. The FE model is evaluated at these training points to obtain the output training data. In order to propagate the variation to the second stage FE model the nodal displacements (\mathbf{u} in x -direction and \mathbf{v} in y -direction), the equivalent plastic strain ($\boldsymbol{\varepsilon}_{eq}^p$, in each integration point) and the stress tensor ($\boldsymbol{\sigma}_{nn}$, in each integration point) are needed as output. Note that due to the plane strain FE analysis two components of the stress tensor $\boldsymbol{\sigma}_{23}$ & $\boldsymbol{\sigma}_{31}$ are zero.

3.2 Reducing the first stage output

In order to construct the snapshot matrix the output data from the FE simulation of the first stage corresponding to sample point $\mathbf{x}^{(k)}$ is stored in a $(2 \cdot N_{nod} + 5 \cdot N_{ip}) = 26592$ by 1 column vector:

$$\mathbf{y}_1^{(k)} = \{\mathbf{u} \quad \mathbf{v} \quad \boldsymbol{\varepsilon}_{eq}^p \quad \boldsymbol{\sigma}_{11} \quad \boldsymbol{\sigma}_{22} \quad \boldsymbol{\sigma}_{33} \quad \boldsymbol{\sigma}_{12}\}^T \quad (10)$$

All column vectors $\mathbf{y}_1^{(k)}$ are collected in the $(2 \cdot N_{nod} + 5 \cdot N_{ip})$ by K snapshot matrix \mathbf{Y}_1 . This snapshot matrix is normalized between -1 and 1 based on the minimum and maximum value in each row, where after the singular value decomposition is applied. The contribution f_k of each singular value s_k to the snapshot matrix is suggested by Skillicorn [17] as:

$$f_k = \frac{s_k^2}{\sum_{i=1}^r s_i^2} \quad (11)$$

Where r is the rank of the snapshot matrix. When all contributions are displayed in a Pareto chart (see Figure 3) on can see that selecting $N_s = 3$ singular values will retain 80% of the information in the snapshot matrix. Hence, the new basis is truncated to 3 singular values only.

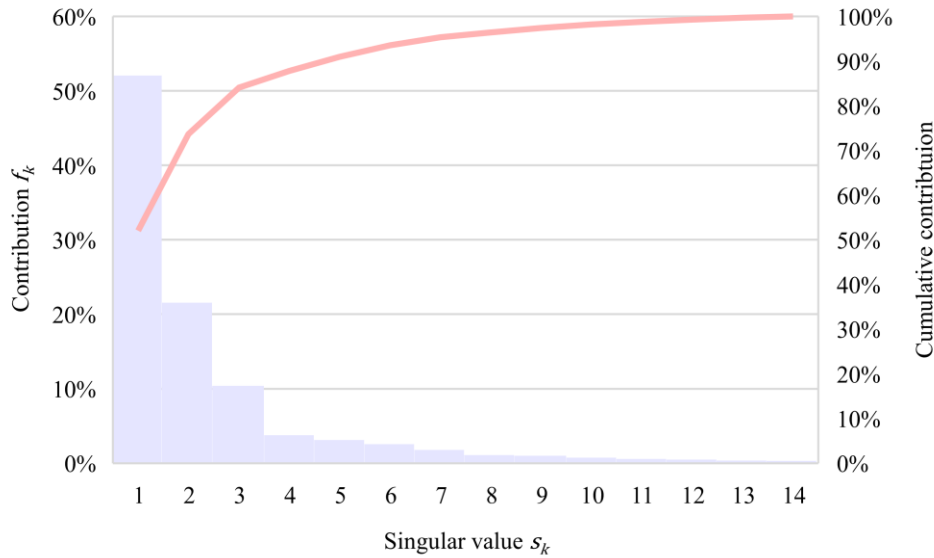


Figure 3: Pareto chart of the contribution of each singular value

After finding the amplitudes as proposed in equation (3) the output the FE simulation corresponding to sample point $\mathbf{x}^{(k)}$ can be approximated by multiplying the left-singular vector with its corresponding amplitude scalar and adding the results:

$$\mathbf{y}_1^{(k)} \approx \boldsymbol{\varphi}_1 a_1^{(k)} + \boldsymbol{\varphi}_2 a_2^{(k)} + \boldsymbol{\varphi}_3 a_3^{(k)} \quad (12)$$

3.3 Building the first stage metamodel

To construct a continuous metamodel of the first stage, the amplitudes corresponding to the training points $\mathbf{a}^{(k)}$ are interpolated using multiquadric radial basis functions (MQ-RBF). A multiquadric radial basis function has the following form:

$$\psi(r) = \sqrt{c_{(k)}^2 + \|\boldsymbol{\theta}(\mathbf{x}^{(k)} - \mathbf{x})\|^2} \quad (13)$$

Resulting in the following SVD MQ-RBF metamodel of the first stage:

$$\hat{\mathbf{y}}_1(\mathbf{x}) = \boldsymbol{\varphi}_1 a_1(\mathbf{x}) + \boldsymbol{\varphi}_2 a_2(\mathbf{x}) + \boldsymbol{\varphi}_3 a_3(\mathbf{x}) \quad (14)$$

To test the quality of the obtained the metamodel a Latin hypercube sampling is used to generate a set of $M = 23$ validation points $\mathbf{x}^{(m)}$. In Figure 4 the displacement field of a validation point is evaluated using both the FE model and the metamodel. In the figure the blue circle is the target, hence the FE model, while the red dot is the result of the metamodel. The displacement field of the metamodel is good agreement with the displacement field of the FE-model. In the zoomed panel the region with the largest deviations is

displayed. In this region, the values from the metamodel are in proximity of the FE-model, however there are still opportunities for further enhancement.

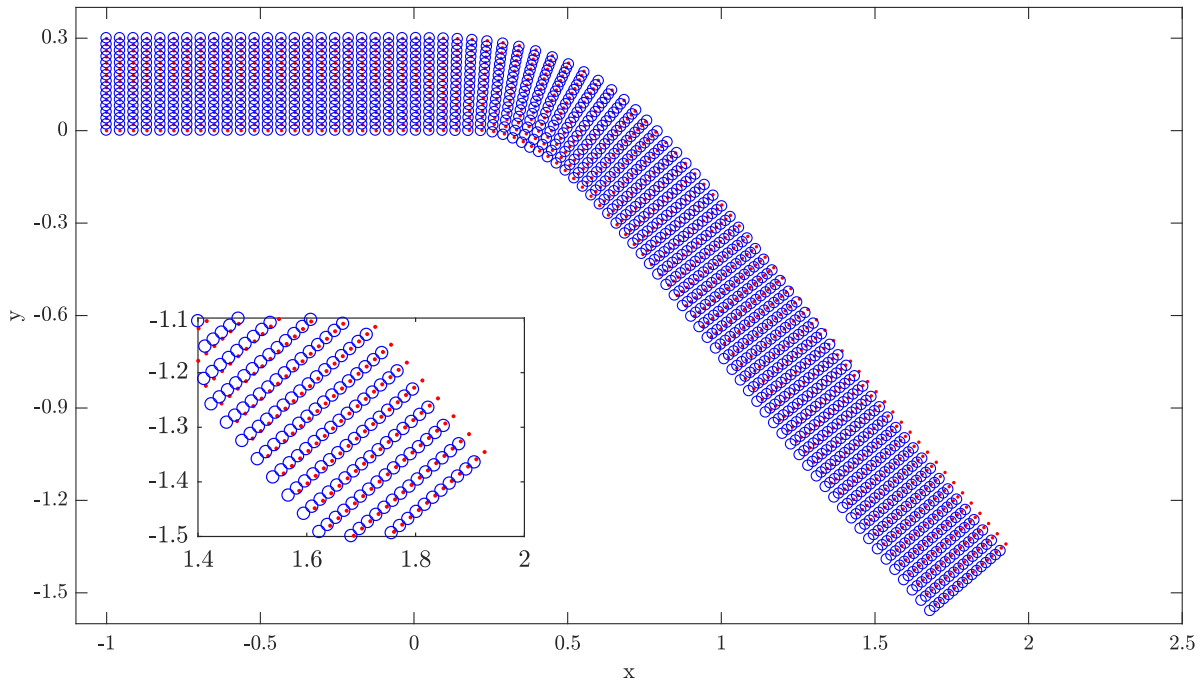


Figure 4: Output of the displacement field $\{\mathbf{u}, \mathbf{v}\}$ from both the first stage SVD MQ-RBF metamodel (\cdot) and the FE model (\circ). The zoomed panel shows the region with the largest RMSE.

A root mean square error (RMSE) can be calculated by subtracting the metamodel evaluated at a validation point $\hat{\mathbf{y}}_1(\mathbf{x}^{(m)})$ from the actual FE results $\mathbf{y}_1^{(m)}$:

$$RMSE = \sqrt{\frac{1}{M} \sum_{m=1}^m \left(\mathbf{y}_1^{(m)} - \hat{\mathbf{y}}_1(\mathbf{x}^{(m)}) \right)^2} \quad (15)$$

The RMSE is calculated for the different types of output data. The relative error in the different types of output data is calculated by dividing the RMSE by the absolute average. All error values are collected in Table 1. Although the relative errors for both σ_{11} and σ_{12} seem extremely large, the RMSE of all stresses is in the same order as the stresses itself. These first stage results will now be propagated to the next stage.

Output	Average value	RMSE	Relative error
\mathbf{u}	-0.1943	0.001166	0.600%
\mathbf{v}	-0.4840	0.001529	0.316%
$\boldsymbol{\varepsilon}_{eq}^p$	0.02776	9.092e-4	3.28%
σ_{11}	-11.54	15.74	136%
σ_{22}	-95.16	12.23	12.9%
σ_{33}	-38.92	12.43	31.9%
σ_{12}	1.936	9.139	472%

Table 1: Error values based on metamodel results of 23 validation points.

3.4 Propagating first stage results to the second stage

The results from the validation points $\mathbf{x}^{(m)}$ presented in the previous section from both the first stage SVD MQ-RBF metamodel and the first stage FE model are propagated to the second stage FE model. Unfortunately some of the second stage FE evaluations failed to converge, resulting in a set of $M = 14$ validation points $\mathbf{x}^{(m)}$ only. In Figure 5 the displacement field of a validation point is evaluated using both the FE model and the metamodel. Again the blue circle is the target, hence the first stage FE model propagated to the second stage FE model, while the red dot is the result of the metamodel propagated to the second stage FE model. Again, the displacement field of the metamodel seems in good agreement with the displacement field of the FE-model. Even in the region with the largest deviations the values from the metamodel are in close proximity of the FE-model.

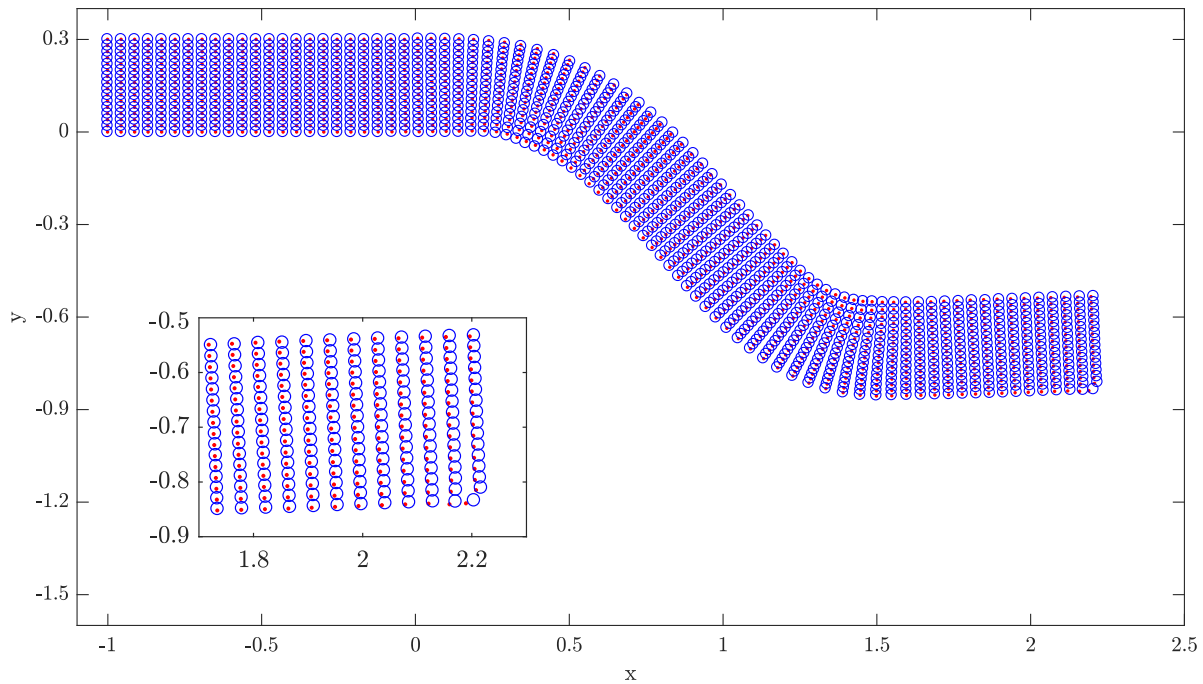


Figure 5: Output of the displacement field $\{\mathbf{u}, \mathbf{v}\}$ from both the first stage SVD MQ-RBF metamodel combined with the second stage FE model (\cdot) and when both stages are modeled using the FE model (\circ). The zoomed panel shows the region with the largest RMSE.

Output	Average value	RMSE	Relative error
\mathbf{u}	-0.1271	0.006360	5.00%
\mathbf{v}	-0.3707	0.01279	3.42%
$\boldsymbol{\varepsilon}_{eq}^p$	0.05891	0.002258	3.83%
$\boldsymbol{\sigma}_{11}$	-12.35	21.20	172%
$\boldsymbol{\sigma}_{22}$	-94.88	15.36	16.19%
$\boldsymbol{\sigma}_{33}$	-77.01	18.61	24.17%
$\boldsymbol{\sigma}_{12}$	-0.4207	11.71	2785%

Table 2: Error values based on propagated results of 14 validation points

The RMSE of the validation points is calculated for the different types of output data of the second stage. All error values are collected in Table 2. The extremely large error in the metamodel of the σ_{12} component of the stress tensor, can be classified as an artificial error. Due to the low average value a change in sign will lead to a large RMSE and therefore a large relative error. The average relative error of the nodal displacements and the equivalent plastic strain is only 2,29% in the first stage and 3,96% in the second stage. Comparing Table 1 and Table 2 one can see that the error in the metamodel will propagate and increase with every stage.

4 Conclusion

The strategy proposed in this work has been used to feasible propagate output data to a subsequent stage. The propagated results after the second stage of both the displacement and equivalent strain fields are in good agreement with the finite element model. The stresses show relatively large deviations.

In future work the same strategy will be used to efficiently describe the second stage output in order to optimize the multi-stage production process.

Acknowledgements

This research project is part of the ‘Region of Smart Factories’ project and is partially funded by the ‘Samenwerkingsverband Noord-Nederland (SNN), Ruimtelijk Economisch Programma’.

References

- [1] M. H. A. Bonte, “Optimization Strategies for Metal Forming Process,” University of Twente, 2007.
- [2] J. H. Wiebenga, “Robust design and optimization of forming processes,” University of Twente, 2014.
- [3] G. Taguchi, *Introduction to Quality Engineering: Designing Quality into Products and Processes*. Quality Resources, 1986.
- [4] M. S. Phadke, *Quality Engineering Using Robust Design*. Prentice Hall, 1989.
- [5] R. Suri and K. Otto, “Manufacturing System Robustness Through Integrated Modeling,” *J. Mech. Des.*, vol. 123, no. 4, p. 630, 2001.
- [6] S. Roy, S. Ghosh, and R. Shivpuri, “A new approach to optimal design of multi-stage metal forming processes with micro genetic algorithms,” *Int. J. Mach. Tools Manuf.*, vol. 37, no. 1, pp. 29–44, 1997.
- [7] H. J. Bong, F. Barlat, J. Lee, M.-G. Lee, and J. H. Kim, “Application of central composite design for optimization of two-stage forming process using ultra-thin ferritic stainless steel,” *Met. Mater. Int.*, vol. 22, no. 2, pp. 276–287, 2016.
- [8] L. Monostori and Z. J. Viharos, “Hybrid, AI- and simulation-supported optimisation of process chains and production plants,” *CIRP Ann. - Manuf. Technol.*, vol. 50, no. 1, pp. 353–356, 2001.
- [9] Y. Abe, K. Mori, and O. Ebihara, “Optimisation of the distribution of wall thickness in the multistage sheet metal forming of wheel disks,” *J. Mater. Process. Technol.*, vol. 125–126, pp. 792–797, 2002.
- [10] B. Denkena and H. Henning, “Multicriteria dimensioning of hard-finishing operations regarding cross-process interdependencies,” *J. Intell. Manuf.*, vol. 23, no. 6, pp. 2333–2342, 2012.
- [11] J. Kusiak, P. Morkisz, P. Oprocha, W. Pietrucha, and Ł. Sztangret, “On Aggregation of Stages in Multi-criteria Optimization of Chain Structured Processes,” in *Lecture Notes in Artificial Intelligence 9692*, vol. Part I, Springer International Publishing Switzerland, 2016, pp. 411–419.
- [12] P. Jarosz *et al.*, “A Methodology for Optimization in Multistage Industrial Processes : A Pilot Study,” *Math. Probl. Eng.*, vol. 2015, 2015.
- [13] D. Steffes-Lai, “Approximation Methods for High Dimensional Simulation Results Parameter Sensitivity Analysis and Propagation of Variations for Process Chains,” University of Cologne, 2014.
- [14] D. Sun, F. Andrieux, and M. Feucht, “Simulation of the process chain from forming to crash taking

- into account stochastic aspects,” *LS-DYNA Forum, Bamb. 2010*, pp. 1–10, 2010.
- [15] X. Du and W. Chen, “Efficient Uncertainty Analysis Methods for Multidisciplinary Robust Design,” *AIAA J.*, vol. 40, no. 3, pp. 545–552, 2002.
- [16] O. Nejadseyfi, H. J. M. Geijselaers, and A. H. Van Den Boogaard, “Efficient calculation of uncertainty propagation with an application in robust optimization of forming processes,” *AIP Conf. Proc.*, vol. 1896, 2017.
- [17] D. Skillicorn, *Understanding Complex Datasets: Data Mining with Matrix Decompositions (Chapman & Hall/Crc Data Mining and Knowledge Discovery Series)*. 2007.
- [18] V. Buljak, “Proper Orthogonal Decomposition and Radial Basis Functions Algorithm for Diagnostic Procedure Based on Inverse Analysis,” *FME Trans.*, vol. 38, no. 3, pp. 129–136, 2010.
- [19] A. Chatterjee, “An introduction to the proper orthogonal decomposition,” *Curr. Sci.*, vol. 78, no. 7, pp. 808–817, 2000.